Industrial Silencers Design

Renato Rocha
renato.a.rocha@tecnico.ulisboa.pt

Instituto Superior Técnico, Universidade de Lisboa, Portugal

November 2018

Abstract

A method to model industrial silencers is developed, based on existing theoretical models for attenuation formulated by other researchers. Among the several existing theories, it was chosen the theory that would take us to the desired solution: ducts lined on two opposite walls with porous material. At the first, the chosen theory is analysed and verified its implementation through a simplified model. Subsequently, through the models and experiences found in literature, the absorption coefficient that appeared on the acoustic material specification sheet given by the supplier was compared with the acoustic properties, propagation coefficient and characteristic impedance, required to calculate the attenuation through the model previously chosen. Finally, the different parameters which were important in the silencers project were studied in order to measure the effect that these caused in the attenuation. Knowing the influence that each characteristic of the silencer has on the obtained attenuation, a procedure was elaborated for the industrial acoustic silencers design.

Keywords: Silencer, noise reduction, attenuation, propagation coefficient, characteristic impedance

1. Introduction

The concern about industrial noise has grown increasingly, and its occurrence is related to several health problems. It becomes important to find solutions to reduce this noise. One of this solutions is to reduce the noise caused by the units of Heating, Ventilation and Air Conditioning (HVAC), which are necessary for the proper operation of the industrial cabin.

From the type of components used, to the method of construction of the noise attenuating ducts, all the characteristics are important when dimensioning a silencer. The conclusions drawn from the studies comparing the different types of silencers have been applied in the aeronautics industry, for example, in the acoustic improvement of the fan and the exhaust duct, so that the noise is attenuated.

2. Background

2.1. Acoustic properties of porous materials

2.1.1. Propagation coefficient and characteristic impedance

Based on experimental results, Delany and Bazley [5] determinated expressions for the characteristic impedance and propagation coefficient, as a function of the sound wave frequency passing through the porous material. Although these equations are quite simple, they present only desired solutions within a short range of frequencies. On the other hand, Allard and Champoux [2] developed the phenomenological model, where they define new expressions for the calculation of the acoustic properties of a porous material. Contrary to Delany and Bazley [5], Allard and Champoux [2] presented valid solutions for low frequencies.

2.1.2. Flow resistivity

Flow resistance is a fundamental parameter in any theory developed with the purpose of studying the porous materials and their applications. As its name implies, this property quantifies the resistance that the porous material offers to the flow that passes through it. The flow resistivity, σ, is the flow resistance per unit of thickness.

2.2. Different porous materials

2.2.1. Locally reacting

The locally reacting model, also known as the point reacting model, is based on materials with high flow resistance, density, porosity and sound absorption. In these porous material, the wave propagation is zero.

Initially, Morse [9] studied the attenuation in two-dimensional, rectangular and circular ducts lined with porous material. One year later, Cremer [3] concluded that the locally reacting model should be used in high density materials, since it allows

to obtain a maximum attenuation peak at reduced damping values.

2.2.2. Bulk reacting

The bulk reaction model is used to describe the sound propagation in ducts lined with porous material, taking into account the sound propagation inside the porous material.

In 1965, Tack and Lambert [10] studied the effects caused by uniform and exponential flow in the study of noise attenuation in isotropic two-dimensional ducts.

Kurze and Vér [8] were the first researchers to analyse the effect of non-isotropic porous material at noise attenuation in rectangular ducts without flow. They conclude that it is necessary to consider the non-isotropic characteristics of the material, especially when acoustic absorbent material with reduced flow resistance are used.

In 1976, Cummings [4] predicts the existence of flow in rectangular and cylindrical three-dimensional ducts lined with porous material. Later on, Frommhold and Mechel [6] presented simplified expressions, based on the Bessel's equations for noise attenuation in three-dimensional rectangular and cylindrical ducts with flow.

3. Theoretical models to determination of the acoustical attenuation

3.1. Silencer characteristics

Figure 1 show the duct geometry, coordinate systems and dimensions, along with those of the perforated facing. The model assumes that the outer walls are rigid, so there is no dissipation of acoustic energy.

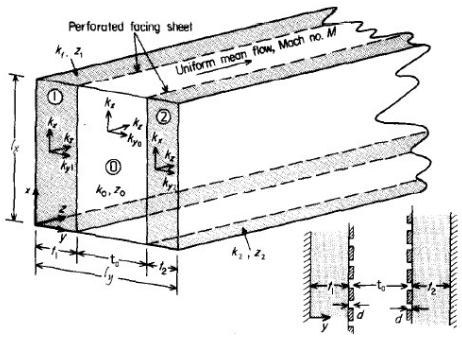

Figure 1: Silencer characteristics. (Adapted from Cummings [4].)

The silencer under study is described by a rectangular geometry duct lined on two opposite walls by porous material. On the inner face of each porous section, there is a perforated sheet. In the conduct center there may be flow, in the positive and negative direction of sound propagation. This cavity was named byairwaye. For convenience, an index, j, will be used for each of the sections:

- 1 and 2 are relative to the two wall liners;
- 0 is relative to the airway.

3.2. Determination of the attenuation

The sound pressure field in duct can be represented by an infinite series of modes or eigenfunctions, given by:

$$p(x,y,z,t) = e^{\mathrm{i}\,\omega t} \sum_{m=0}^{\infty}\sum_{n=0}^{\infty} \Psi^{mn}(x,y) e^{-\mathrm{i}\,z k_z^{mn}}, \quad (1)$$

where p is the acoustic pressure, Ψ is an eigenfunction, k_z is the axial wavenumber and ω is the angular frequency.

The real part of equation 1 corresponds to the sound signal amplitude, while the complex part establishes the oscillatory character of the signal.

Attenuation is defined as the decrease in the sound pressure level(SPL) along the length of duct. Thus, the attenuation in dB per unit length of duct, $|z|$, is given by:

$$\Theta = -8.6858\,\mathrm{Im}\,(k_z)\,, \quad (2)$$

3.3. Alan Cummings Model

From the literature presented above, it was chosen the theory developed by Cummings [4]. Since that model considers bulk reaction materials (usually used in the manufacture of industrial silencers), rectangular three-dimensional conducts (intended geometry) and perforated sheets (used for protection of the porous material).

3.3.1. Caracterization of the sound pressure field

Ignoring the superscripts mn in equation (1), the function Ψ is given by the sum of different eigenfunctions relative to each duct section. These functions Ψ_j are given by the product of two functions characterized by sound propagation in the x and y-direction:

$$\Psi_j = X_j(x) Y_j(y). \quad (3)$$

The hard walls boundary coundition at $x = 0$ and $x = l_x$ imposed a zero normal pressure gradient at

these coordinates. A possible function X_j with null gradient at $x = 0$ and $x = l_x$ is:

$$X_j(x) = \cos(k_x x), \tag{4}$$

where k_x is the wavenumber in the x-direction, defined by $k_x = m\pi/l_x$, where l_x is the length of the duct, also in the x-direction.

Regarding the y-direction, there are several boundary conditions: discontinuities between each different section, and rigid wall at $y = 0$ and $y = l_y$. Due to these boundary conditions, the expressions for each Y function are more complicated to obtain. Nevertheless, Cummings [4] proposes the following expressions:

$$Y_1(y) = p_1 \cos(k_{y1} y), \tag{5}$$

$$Y_2(y) = p_2 \left[\cos(k_{y2} y) + \tan(k_{y2} l_y) \sin(k_{y2} y)\right], \tag{6}$$

$$Y_0(y) = p_0 \left[\cos(k_{y0} y) + B \sin(k_{y0} y)\right], \tag{7}$$

where p_j and k_{yj} are the mean acoustic pressure and the wavenumber in the y-direction (in the j section of the duct) and l_y is the duct dimension in the y-direction.

In addition to the boundary conditions mentioned above, the displacement of the surface of the perforated sheets in contact with the porous section should be equal to the displacement of the adjacent air particles. This displacement is called the displacement impedance, ε. The two boundary conditions referred, can be mathematically written by:

$$\varepsilon_0(t_1 + d) = \varepsilon_1(t_1 + d), \tag{8}$$

$$\varepsilon_0(t_1 + t_0 + d) = \varepsilon_2(t_1 + t_0 + d), \tag{9}$$

where t_j is the width of the j section of the conduct and d the thickness of the perforated sheet.

Through the previous boundary conditions, it is possible to get the formulation presented by Cummings [4]:

$$\begin{aligned} &(D_1 \tan[k_{y0}(t_1 + d)] - E)\times \\ &\times(E \tan[k_{y0}(t_1 + t_0 + d)] + D_2) - \\ &-(D_2 \tan[k_{y0}(t_1 + t_0 + d)] - E)\times \\ &\times(E \tan[k_{y0}(t_1 + d)] + D_1) = 0, \end{aligned} \tag{10}$$

where D_1, D_2 and E are given by:

$$D_1 = \mathrm{i}\,\frac{z_1}{z_0}\frac{k_1}{k_{y1}} \cot(k_{y1} t_1) - \zeta_{h1}, \tag{11}$$

$$D_2 = -\,\mathrm{i}\,\frac{z_2}{z_0}\frac{k_2}{k_{y2}} \cot(k_{y2} t_2) + \zeta_{h2}, \tag{12}$$

$$E = \mathrm{i}\,\frac{(k_0 - M k_z)^2}{k_0 k_{y0}}, \tag{13}$$

where z_j, k_j and ζ_{hj} are the characteristic impedance, wavenumber and non-dimensional impedance in the perforated sheet adjacent to the porous material of section 1 or 2, respectively, and M is the mean Mach number of the flow that passes through the duct, given by $M = U/c_0$.

The characteristic impedance and the wavenumber of the section of the airway, these properties are given, respectively, by:

$$z_0 = \rho_0 c_0, \tag{14}$$

$$k_0 = \frac{\omega}{c_0}, \tag{15}$$

where ρ_0 and c_0 are the fluid density and the mean flow velocity.

Cummings [4] defines the non-dimensional impedance ζ_{hj} by:

$$\zeta_{hj} = \frac{\mathrm{i}\,k_0}{Q}\left[\delta\left(\mathrm{H}\left(1 - |U|\right) + \frac{z_1}{z_0}\frac{k_1}{k_0}\right) + d\right], \tag{16}$$

where Q is the "porosity" of the perforate, δ is the mass end correction given by 17 and U is the mean flow velocity.

The mass end correction for round circles given by Ingard [7] may be approximated by a two-part curve, as follow:

$$\delta = \begin{cases} 0.85 r_0 \left(1 - 2.34\dfrac{r_0}{l}\right), & 0 < \dfrac{r_0}{l} \leq 0.25, \\ 0.668 r_0 \left(1 - 1.9\dfrac{r_0}{l}\right), & 0.25 < \dfrac{r_0}{l} < 0.5, \end{cases} \tag{17}$$

where r_0 is perforation radius and l is the pitch.

By simplifying the wave equation, $\left(D^2/Dt^2 - c_0^2 \nabla^2\right) p = 0$, calculated for the pressure in the three sections of the duct, the wavenumbers in the x, y, and z direction are related to the wavenumbers of each material by the following expressions:

$$(k_0 - M k_z)^2 - k_z^2 - k_x^2 - k_{y0}^2 = 0. \tag{18}$$

$$k_1^2 - k_z^2 - k_x^2 - k_{y1}^2 = 0, \tag{19}$$

$$k_2^2 - k_z^2 - k_x^2 - k_{y2}^2 = 0. \tag{20}$$

3.3.2. Determination of the axial wavenumber

Equations (10), (18), (19) and (20) compose a 4 by 4 system of equations, where k_z, k_{y1}, k_{y2} and k_{y0} are the unknowns. There are several methods of solving this problem, still, it was chosen to solve

equations (18), (19) and (20) in order to k_z, k_{y1} and k_{y2}, respectively:

$$k_{y1} = \sqrt{k_1^2 - k_z^2 - k_x^2}, \tag{21}$$

$$k_{y2} = \sqrt{k_2^2 - k_z^2 - k_x^2}, \tag{22}$$

$$k_z = \frac{Mk_0 - \sqrt{(Mk_0)^2 - (M-1)\left(k_0^2 - k_x^2 - k_{y0}^2\right)}}{M-1}. \tag{23}$$

In this way, it was obtained a proper equation in k_{y0}, which can be solved numerically only by replacing equations (21), (22) and (23) in the equation (10). This equation will be solved by the Newton-Raphson method. This method needs an initial solution that is close to the expected result, otherwise the final solution will present a high error.

In order to obtain an initial value of the iterative method, three assumptions will be stablished:

- the existence of perforated sheets is neglected;
- the admittance, η, is the inverse of displacement impedance;
- reduced admittance values.

Therefore, the admittance on the surface of the porous sections in contact with the airway, η_1 and η_2, are obtained through the following equations:

$$\eta_1\left(t_1\right) = -\,\mathrm{i}\,\frac{z_0}{z_1}\frac{k_{y1}}{k_1}\tan(k_{y1}t_1), \tag{24}$$

$$\eta_2(t_1 + t_0) = \mathrm{i}\,\frac{z_0}{z_2}\frac{k_{y2}}{k_2}\tan(k_{y2}t_2). \tag{25}$$

The admittances of the porous material at the discontinuity surface will be equalized with the respective fluid admittance, contained in the airway section at that discontinuity coordinate. After applying these boundary conditions, and considering reduced admittance values, Cummings [4] obtained the initial wavenumber in the y-direction given by:

$$k_{y0} \approx \begin{cases} \left(1 - M\dfrac{k_z}{k_0}\right)\sqrt{\mathrm{i}\,k_0\dfrac{\eta_1+\eta_2}{t_0}}, & n = 0, \\ \dfrac{n\pi}{t_0} + \mathrm{i}\left(1 - M\dfrac{k_z}{k_0}\right)^2\dfrac{\eta_1+\eta_2}{2n\pi}, & n > 0. \end{cases} \tag{26}$$

For the fundamental mode, the initial guess is obtained for the lowest frequency of the frequency range to be calculated, obtaining the wavenumber for that frequency by the Newton-Raphson method. The frequency was the increased by a small amount, and the previously calculated wavenumbers used in the initial guess.

3.4. Validation of the A. Cummings model

In order to validate the Cummings [4] model, it was also implemented the model presented by Frommhold and Mechel [6]. This is a simplified model in which have been presented simpler expressions for the calculation of the wavenumber, k_z.

Frommhold and Mechel [6] do not have predicted the existence of perforated sheets and have considered equal opposite absorbent walls. In Figure 2 it was compared the Cummings [4] model with Frommhold and Mechel [6] model, for two different speeds, $\{0, 20\}\,\mathrm{m\,s^{-1}}$.

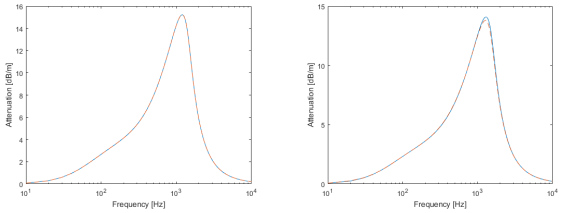

(a) $U = 0\,\mathrm{m\,s^{-1}}$ (b) $U = 20\,\mathrm{m\,s^{-1}}$

Figure 2: Comparation between the models of Cummings [4] and Frommhold and Mechel [6] model: $t_0 = 0.35\,\mathrm{m}$; $t_1 = t_2 = 0.175\,\mathrm{m}$; $\sigma = 30 \times 10^3\,\mathrm{kg\,s^{-1}\,m^{-3}}$. ——, A. Cummings model; – –, W. Frommhold e F. Mechel. model

In figure 2, it is possible to verify that the data calculated through each model is very close. As expected, the results obtained for reduced velocities, figures 2(a-b), are very close, with the maximum error verified being 0.1% and 0.8%, respectively. In the duct without flow, figure 2(a), a maximum error of 0.1% is obtained, while for the velocity of $20\,\mathrm{m\,s^{-1}}$ it is obtained a maximum error of 3%. These results are in agreement with the expected, since the error is smaller for reduced speeds.

Therefore, the Cummings [4] model was successfully implemented and can be used to study attenuation in duct lined on two opposite walls with porous material.

3.5. Determination of the acoustical properties of porous material

As said before, the characteristic impedance and wavenumber will be determinated in this section. Allard and Champoux [2] defined this parameters by the following expressions:

$$z = \sqrt{\rho_d K_d}, \tag{27}$$

$$k = 2\pi f\sqrt{\frac{\rho_d}{K_d}}, \tag{28}$$

where ρ_d is dynamic density and K_d is dynamic bulc modulus, given by equations (29) and (30), respectively.

The dynamic density, ρ_d, which takes into account the inertial and the viscous forces per unit volume of the air in the material, s given by:

$$\rho_d(f/\sigma) = \rho_0 \left[1 + \frac{G_1(f/\sigma)}{\mathrm{i}\,2\pi}\frac{\sigma}{\rho_0 f}\right] \tag{29}$$

where $G_1(f/\sigma)$ is a function defined by Allard and Champoux [2] and given by an equation (31).

The dynamic bulk modulus, K_d, which relates the divergence of the averaged molecular displacement of the air to the averaged variation of the pressure, is given by:

$$K_d(f/\sigma) = \gamma p_0 \left(\gamma - \frac{\gamma - 1}{1 + (1/\mathrm{i}\,8\pi N_{pr})(\sigma/\rho_0 f)G_2(f/\sigma)}\right)^{-1} \tag{30}$$

where N_{pr} is Prandtl number given by $N_{pr} = c_p\mu/\kappa$, μ is dynamic viscosity, κ is thermal conductivity and $G_2(f/\sigma)$ is a function defined by [2] and given by (32).

$G_1(f/\sigma)$ and $G_2(f/\sigma)$ defined by Allard and Champoux [2] are given by:

$$G_1(f/\sigma) = \sqrt{1 + \mathrm{i}\,\pi\frac{\rho_0 f}{\sigma}}, \tag{31}$$

$$G_2(f/\sigma) = G_1(f/\sigma)\frac{\rho_0 f}{\sigma}4N_{pr}. \tag{32}$$

3.6. Cálculo da resistência específica ao escoamento

The acoustic properties of the porous material depend on the specific flow resistivity. Ideally, flow resistivity would be obtained experimentally, either directly, through the methods referred in the section 2.1.2, or indirectly, through experimental determination of the characteristic impedance using, for example, the procedures defined by the standard EN ISO 10534-2 [1]. After obtaining the characteristic impedance, the flow resistivity and, later, the wavenumber can be inferred through the models presented by Allard and Champoux [2].

If it becomes impossible to obtain the flow resistivity, the nominal characteristics of the material supplied by the manufacturer must be used. Of these, the most relevant is the absorption coefficient given for various frequencies and for various material thicknesses, e.

On the other hand, the theoretical absorption coefficient α_n is given by:

$$\alpha_n = 1 - \left|\frac{z\coth(\mathrm{i}\,ke) - \rho_0 c_0}{z\coth(\mathrm{i}\,ke) + \rho_0 c_0}\right|^2. \tag{33}$$

Given that the nominal characteristics given by the manufactorer were obtained experimentally, it is necessary to adjust this values to the best curve defined by the equation (33). Then, it will be used the method of least squares, where the flow resistivity is the design variable. The purpose of this method is to obtain the flow resistivity, which minimizes the sum of the squares of the residuals given by the difference of experimental absorption coefficients and the theoretical absorption coefficients given by the equation (33). Therefore, the minimizer equation is defined by:

$$E = \sqrt{\sum_{i=0}^{q}(\alpha_e(f_i) - \alpha_n(f_i))^2} \tag{34}$$

where q is the number of absorption coefficients measured for a given thickness material.

4. Acustic attenuation in function of the silencer characteristics

4.1. Choice of parameters

Since the calculation of the attenuation depends on a large number of parameters, it is necessary to choose which parameters to analyse and their limits of variation. In this way, the effects of these parameters will be studied, considering that the remaining parameters are constants.

The effect of varying the dimensions of the conduct should be studied. The three ways of varying the total width of the conduct are:

a) constant airway width and variable porous sections thicknesses;

b) constant porous sections thicknesses and variable airway width;

c) variable airway width and porous sections thicknesses.

The flow resistivity is a characteristic of the selected porous material, therefore, it must also be a property to be studied. This property does not depend on other properties, so it is an interesting amount to analyse.

The velocity of the flow inside a ventilation duct can be significant, so it is necessary to estimate the effect of this variable on the attenuation obtained.

The existence of perforated sheets between each porous section and the airway will also be a variable under study.

In all subsequent analysis, the ambient conditions were considered: a temperature of 20 °C and a pressure of 101.325 kPa.

4.2. Effects of the dimensions of a symmetrical silencer

The effects of the width of the airway and the thickness of the porous sections in the attenuation of sound waves can be studied in several ways: keeping one of these properties constant and the other variable (total width of the duct is variable), or by varying these two variables (the total width of the duct is variable or constant depending on the variation of these two properties). Since there are very different ways of varying the dimensions of an attenuating duct, it is important to define a designated amount of space factor, $SF = t_0/l_y$.

In this way, three different situations were studied:

(a) varying the thickness of the porous sections 1 and 2, keeping the width of the airway constant;

(b) varying the width of the airway, remaining the thicknesses of the porous sections 1 and 2 constant;

(c) varying airway width and porous sections 1 and 2 thicknesses so that the width of the duct remained constant;

Initially, the effects of the variation of the porous section thickness were studied, considering the width of the constant airway, in the value of 0.35 m. Figure 3 shows this analysis in ducts with a factor of spacing of 25%, 50% and 75% under zero flow velocity. Likewise, figure 4 represents this analysis for variable airway widths, rather than variable porous sections thicknesses.

The effect of the space factor on ducts of the same width was analysed for ducts with 0.70 m of total width under zero flow velocity. Thus, several different ducts with a factor of spacing of 25%, 50% and 75% were studied. The graphs of figure 5 show the effect that the space factor causes in the attenuation obtained.

Figure 3 shows that the thickness of the porous material strongly influences the attenuation of low frequency sound waves, whereas the high frequency wave attenuation does not vary with the thickness of the porous material. As the space factor increases and the width of the airway is constant, the thickness of the porous material decreases. Thus, for smaller porous sections thicknesses, the attenuation of low frequency sound waves is smaller. In contrast, the effect at high frequencies is practically zero, so varying the thickness of the porous material within the order of magnitude under study, does not affect the attenuation of high frequency sound waves.

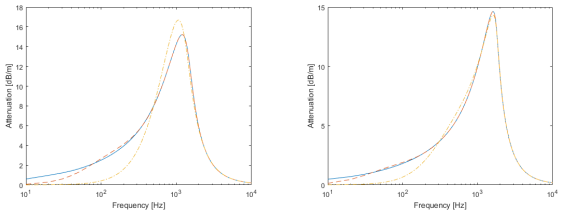

(a) $\sigma = 30 \times 10^3\,\mathrm{kg\,s^{-1}\,m^{-3}}$ (b) $\sigma = 60 \times 10^3\,\mathrm{kg\,s^{-1}\,m^{-3}}$

Figure 3: Effect of the dimensions of a symmetrical silencer in sound wave attenuation: $t_0 = 0.35\,\mathrm{m}$. ——, $SF = 25\%$; – –, $SF = 50\%$; – . – ., $SF = 75\%$.

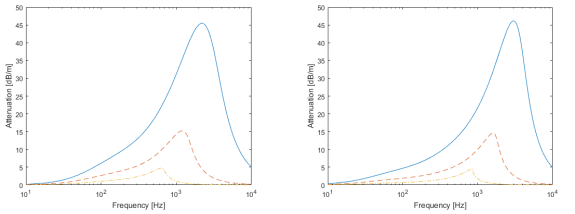

(a) $\sigma = 30 \times 10^3\,\mathrm{kg\,s^{-1}\,m^{-3}}$ (b) $\sigma = 60 \times 10^3\,\mathrm{kg\,s^{-1}\,m^{-3}}$

Figure 4: Effect of the dimensions of a symmetrical silencer in sound wave attenuation: $t_1 = t_2 = 0.175\,\mathrm{m}$. ——, $SF = 25\%$; – –, $SF = 50\%$; – . – ., $SF = 75\%$.

Figures 4 and 5 show that the effect of the width of the airway overlaps the effects of the other characteristics under study. From these figures we conclude that the attenuation and width of the airway vary inversely.

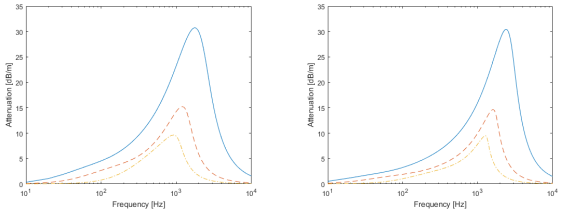

(a) $\sigma = 30 \times 10^3\,\mathrm{kg\,s^{-1}\,m^{-3}}$ (b) $\sigma = 60 \times 10^3\,\mathrm{kg\,s^{-1}\,m^{-3}}$

Figure 5: Effect of the dimensions of a symmetrical silencer in sound wave attenuation: $l_y = 0.70\,\mathrm{m}$. ——, $SF = 25\%$; – –, $SF = 50\%$; – . – ., $SF = 75\%$.

In the graph of figure 3(a), the maximum attenuation obtained for the duct with a space

factor of 75% is greater than the maximum attenuation obtained for the ducts with less space factor. Note that, increasing the space factor by decreasing the thickness of the porous material, when keeping the width of the airway constant, implies a decrease in the size of the duct.

After analysing ducts with the same dimension as the smaller ducts and constituted by porous materials with upper flow resistivity, it is was possible to conclude that this "jump" in the maximum obtained attenuation depends on the silencer versus flow resistivity considered. The greater the flow resistivity, the smaller the duct width will have to be for this effect to occur.

4.3. Effects of the flow resistivity

For this analysis it was again considered an attenuating duct under zero flow velocity, with an airway of 0.35 m width and space factor of 50%.

The effect of the flow resistivity was evaluated by taking three different values for this property, $\{10,\ 30,\ 60\} \times 10^3 \mathrm{kg\,s^{-1}\,m^{-3}}$. These values are within the range of values that can be obtained with both rock and glass wool, between $2 \times 10^3\,\mathrm{kg\,s^{-1}\,m^{-3}}$ and $80 \times 10^3\,\mathrm{kg\,s^{-1}\,m^{-3}}$.

Since the flow resistivity characterizes the difficulty of the flow in passing through the porous material, the attenuated range is expected to be higher for ducts with low flow resistivity porous lining.

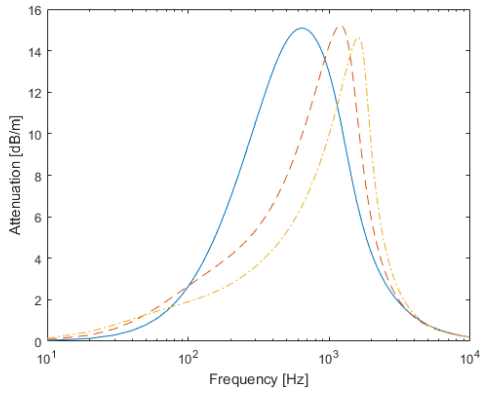

Figure 6: Effect of the flow resistivity in sound wave attenuation, considering ducts with space factor of 50%: $t_0 = 0.35\,\mathrm{m}$; $t_1 = t_2 = 0.175\,\mathrm{m}$. ——, $\sigma = 10 \times 10^3\,\mathrm{kg\,s^{-1}\,m^{-3}}$; – –, $\sigma = 30 \times 10^3\,\mathrm{kg\,s^{-1}\,m^{-3}}$; – . – ., $\sigma = 60 \times 10^3\,\mathrm{kg\,s^{-1}\,m^{-3}}$.

Figure 6 confirms the expected effect given that there is a larger attenuated range for porous materials with less flow resistivity. In addition to this effect, smaller flow resistivity is found to attenuate lower frequency sound waves, whereas higher values of flow resistivity attenuate higher frequency sound waves. Lastly, it is found that the maximum attenuation varies little with the flow resistivity.

The results obtained show that the selection of the porous material with an appropriate flow resistivity allows adjusting the attenuated frequency range.

4.4. Effects of mean flow velocity

In order to evaluate the effect of the mena flow velocity on the attenuation, it was considered an attenuating duct with an airway width of 0.35 m and a space factor of 50%. As for the porous material, it had a flow resistivity of $30 \times 10^3\,\mathrm{kg\,s^{-1}\,m^{-3}}$.

The attenuation determination was made for velocities of $\{-5,\ 5,\ 20,\ 40\}\mathrm{m\,s^{-1}}$. Positive velocities correspond to propagations in the flow direction, whereas negative velocities correspond to the propagations in the opposite direction.

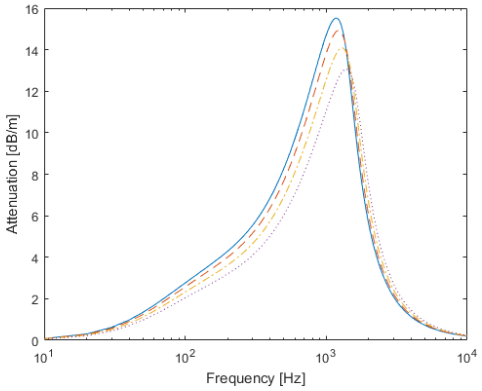

Figure 7: Effect of the mean flow velocity in sound wave attenuation, considering ducts with space factor of 50%: $t_0 = 0.35\,\mathrm{m}$; $t_1 = t_2 = 0.175\,\mathrm{m}$; $\sigma = 30 \times 10^3\,\mathrm{kg\,s^{-1}\,m^{-3}}$. ——, $U = -5\,\mathrm{m\,s^{-1}}$; – –, $U = 5\,\mathrm{m\,s^{-1}}$; – . – ., $U = 20\,\mathrm{m\,s^{-1}}$; ....., $U = 40\,\mathrm{m\,s^{-1}}$.

In the figure 7, it is verified that the increase in velocity decreases the attenuation for low frequency waves. There is a frequency from which this effect is reversed, and the attenuation of sound waves is greater at higher velocities. It is also observed that the frequency which maximizes the attenuation, increases with the flow velocity, although the value of the maximum attenuation decreases.

4.5. Effects of the perforate sheets

In order to analyse the effect of the perforated sheet, it was compared an attenuator without perforated sheets with various attenuators with perforated

sheets different from 1.27 mm of thickness. Three different sizes of perforations were analysed: 1.5 mm, 1 mm and 0.5 mm, that is, perforated sheets with 35.7%, 15.9% and 4% of open area fraction, respectively.

Initially, it was analysed four attenuating ducts without flow and with a 50% space factor: airway widths of 0.35 m and 0.175 m, and porous materials with flow resistivity of $10 \times 10^3\,\mathrm{kg\,s^{-1}\,m^{-3}}$ and $30 \times 10^3\,\mathrm{kg\,s^{-1}\,m^{-3}}$.

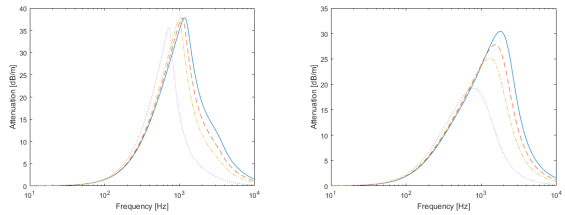

(a) $\sigma = 10 \times 10^3\,\mathrm{kg\,s^{-1}\,m^{-3}}$ (b) $\sigma = 30 \times 10^3\,\mathrm{kg\,s^{-1}\,m^{-3}}$

Figure 8: Effect of the perforate sheets in sound wave attenuation: $U = 0\,\mathrm{m\,s^{-1}}$; $t_0 = 0.175\,\mathrm{m}$; $t_1 = t_2 = 0.0875\,\mathrm{m}$. ——, Without perforate sheets; – –, With perforate sheets: $r_0 = 1.5\,\mathrm{mm}$; – . – ., With perforate sheets: $r_0 = 1\,\mathrm{mm}$; ....., With perforate sheets:: $r_0 = 0.5\,\mathrm{mm}$.

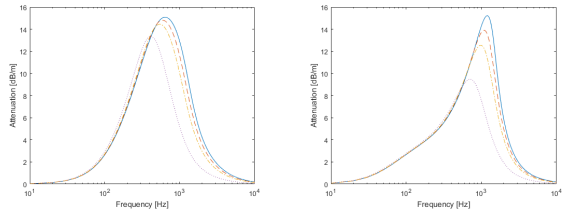

(a) $\sigma = 10 \times 10^3\,\mathrm{kg\,s^{-1}\,m^{-3}}$ (b) $\sigma = 30 \times 10^3\,\mathrm{kg\,s^{-1}\,m^{-3}}$

Figure 9: Effect of the perforate sheets in sound wave attenuation: $U = 0\,\mathrm{m\,s^{-1}}$; $t_0 = 0.35\,\mathrm{m}$; $t_1 = t_2 = 0.175\,\mathrm{m}$. ——, Without perforate sheets; – –, With perforate sheets: $r_0 = 1.5\,\mathrm{mm}$; – . – ., With perforate sheets: $r_0 = 1\,\mathrm{mm}$; ....., With perforate sheets:: $r_0 = 0.5\,\mathrm{mm}$.

In the figures 8 e 9, it is verified that the addition of perforated sheets increases the attenuation of the sound waves with lower frequencies, implying a great decrease of attenuation for high frequencies. These two phenomena (for low and high frequencies) becomes more intense, the smaller the radius of the perforation. In a limit situation where the radius of the perforations decreases to zero, the sheet approaches a hard wall and the attenuation within that duct is zero .

It can still be concluded that, for perforated sheets with elevated area fraction, the value of the obtained attenuation is close to the value of attenuation that would be obtained using the same silencer without perforated sheets.

Finally, it was compared the effect of perforated sheets in silencers with $20\,\mathrm{m\,s^{-1}}$of flow mean velocity, using only two of the silencers studied with zero flow velocity.

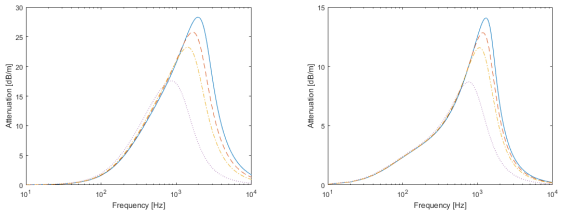

(a) $t_0 = 0.175\,\mathrm{m}$; $t_1 = t_2 = 0.0875\,\mathrm{m}$ (b) $t_0 = 0.35\,\mathrm{m}$; $t_1 = t_2 = 0.175\,\mathrm{m}$

Figure 10: Effect of the perforate sheets in sound wave attenuation: $U = 20\,\mathrm{m\,s^{-1}}$; $\sigma = 30 \times 10^3\,\mathrm{kg\,s^{-1}\,m^{-3}}$. ——, Without perforate sheets; – –, With perforate sheets: $r_0 = 1.5\,\mathrm{mm}$; – . – ., With perforate sheets: $r_0 = 1\,\mathrm{mm}$; ....., With perforate sheets:: $r_0 = 0.5\,\mathrm{mm}$.

Comparing figure 8(b) with figure 10(a) and figure 9(b) with figure 10(b, it is possible to verify that the effect of the perforated sheet on the attenuation is similar. The decrease in the maximum attenuation observed in the figure 10 is due to the presence of flow. It should be noted that this effect has already been verified in section 4.4.

4.6. Effects of the dimensions of an asymmetric silencer

In this section it will be studied the attenuation behaviour in attenuating ducts with different thicknesses for the porous section 1 and 2. It was carried out the study of three different situations:

(a) varying the thickness of the porous section 2, keeping constant the widths of both the airway and the porous section 1;

(b) varying the thickness of the porous sections 1 and 2, remaining constant the width of both the airway constant;

(c) varying airway width and porous section 2 thickness, remaining constant the widths of both the porous section 1 and the duct.

In these three cases it was considered zero flow velocity and flow resistivity of $\sigma = 30 \times 10^3\,\mathrm{kg\,s^{-1}\,m^{-3}}$. It was taken into account three different dimensions for the width of the porous section 2: 0.175 m, 0.0875 m and 0.0437 m.

In the first analysis, figure 11, it was considered a porous section 1 thickness of 0.175 m, and an airway width 0.35 m. In the second case, the thickness of the porous section 1 was increased so that the total width of the duct remained constant, that is, it was considered widths of the porous section 1 of 0.175 m, 0.2625 m and 0.3062 m, figure 12. Similarly, figure 13 represents the analysis of the total width of the duct, which remains constant, but considering a variation of the airway thickness of 0.35 m, 0.4375 m and 0.4812 m, instead of a variation of the porous section 1 thickness.

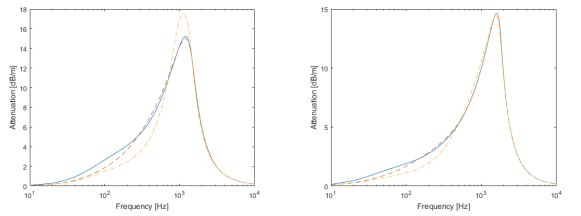

(a) $\sigma = 30 \times 10^3\,\mathrm{kg\,s^{-1}\,m^{-3}}$ (b) $\sigma = 60 \times 10^3\,\mathrm{kg\,s^{-1}\,m^{-3}}$

Figure 11: Effect of the dimensions of a asymmetrical silencer in sound wave attenuation: $t_0 = 0.35\,\mathrm{m}$; $t_1 = 0.175\,\mathrm{m}$. ——, $t_2 = 0.175$; – –, $t_2 = 0.0875$; – . – ., $t_2 = 0.0437$.

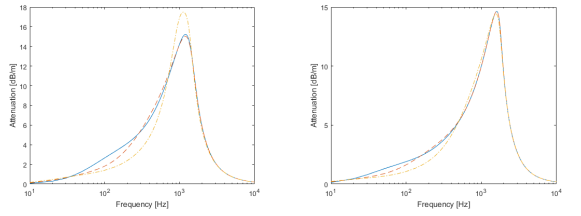

(a) $\sigma = 30 \times 10^3\,\mathrm{kg\,s^{-1}\,m^{-3}}$ (b) $\sigma = 60 \times 10^3\,\mathrm{kg\,s^{-1}\,m^{-3}}$

Figure 12: Effect of the dimensions of a assymmetrical silencer in sound wave attenuation: $t_0 = 0.35\,\mathrm{m}$; $l_y = 0.70\,\mathrm{m}$. ——, $t_2 = 0.175$; – –, $t_2 = 0.0875$; – . – ., $t_2 = 0.0437$.

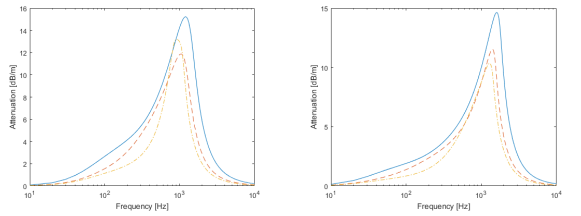

(a) $\sigma = 30 \times 10^3\,\mathrm{kg\,s^{-1}\,m^{-3}}$ (b) $\sigma = 60 \times 10^3\,\mathrm{kg\,s^{-1}\,m^{-3}}$

Figure 13: Effect of the dimensions of a assymmetrical silencer in sound wave attenuation: $t_1 = 0.175\,\mathrm{m}$; $l_y = 0.70\,\mathrm{m}$. ——, $t_2 = 0.175$; – –, $t_2 = 0.0875$; – . – ., $t_2 = 0.0437$.

By comparing the graphs of the figures 11 and 12 with the graphs of the figure 3, it is verified that the obtained attenuation as the thickness of the porous section 2 decreases, is the same as that obtained when the thickness of the porous sections 1 and 2 is decreased by the same value. A detailed analysis of the graphs shows that there is a small difference in the attenuation of lower frequency sound waves, which is greater when the thickness of the porous section 1 does not increases while decreasing the thickness of the porous section 2. In this way, it can be concluded that, in the overall frequency band, the attenuation obtained is independent of the larger porous material thickness.

The attenuation behaviour when the width of the airway increases against the decrease in the thickness of the porous section 2 can be seen in the graphs of figure 13. In this figure, the data obtained is inconclusive regarding the properties under study, since the effect of the airway width exceeds the effect of varying the porous sections thickness.

The maximum attenuation for small ducts will again appear for a flow resistivity of $30 \times 10^3\,\mathrm{kg\,s^{-1}\,m^{-3}}$, figures 11(a), 12(a) and 13(a). This effect is also present in the section 3(a) and is similar to the effect referred to in the section 4.2.

4.7. Procedure for the design of the acoustic silencer

After the evaluation of the effect caused by the essential variables on the silencer design, it is possible to enumerate the steps necessary to project a silencer.

The silencer design should be based on the following phases:

1. calculating the attenuation required for the frequency band in which there is noise to be attenuated;
2. selection of the material with specific flow resistivity so that the frequency of the maximum attenuation corresponds to the frequency of the desired one, shall be selected;
3. choosing the widts of airway and porous sections so that the maximum attenuated value is the expected value;
4. if there is a mean flow velocity inside the duct or there is perforated sheets, the influence of that characteiristics must be calculated and the airway width must be adjusted considering the existence of flow;

5. if the attenuation obtained is the desired attenuation, the project is concluded, otherwise, you should go back to step 2 and change the necessary parameters.

5. Conclusions

The Cummings [4] model, chosen to calculate sound attenuation in ducts lined on two opposite walls with porous material, was implemented successfully and presented theoretical results close to the results obtained by the model of Frommhold and Mechel [6].

It was also related the acoustic performance of a porous material supplied by the manufacturers, with the necessary properties for the determination of the attenuation, characteristic impedance and propagation coefficient. This relationship was achieved through the model of Allard and Champoux [2].

It was analysed several properties to be considered when designing silencers, and the effect of their variation on the attenuation achieved. From the analysed properties, the flow resistivity (type of material) and the airway width are the properties that have the most influence on the attenuation obtained. The type of porous material dictates which band frequency will be the most attenuated, while the airway width affects the expected attenuation value. In addition to these parameters, it is important to consider the flow velocity, since the existence of this one in the propagation direction reduces the expected attenuation. It was also concluded that the thickness of the porous material influences the low frequencies attenuation. As a result of this analysis, the use of perforated sheets does not always add clear benefits to noise attenuation, but must be considered depending on the purpose of the silencer.

It should be noted that the method used to determinate the attenuation caused by rectangular silencers was subjected to some simplifications, which were explained during the development of the dissertation. However, these simplifications should not affect relevantly the expected results, since the purpose of this work is the design of industrial silencers.

In the future, industrial acoustic silencers should be tested in laboratory and compared with the results obtained in this work. These tests should be done in an anechoic chamber. In addition, the same tests can be performed in a wind tunnel in order to verify the effects of the flow on the obtained attenuation. Further geometries of silencers can be studied, for example, rectangular silencers with multiple airways or circular silencers, so that it can be determined the advantages of using these attenuating ducts compared to the rectangular ones with an airway.

Acknowledgements

To my teachers and supervisors João Oliveira and Filipe Cunha for their guidance and patience, without whose this dissertation would not be possible. To my family, friends and girlfriend for their love and support.

References

[1] Determination of sound absorption coefficient and impedance in impedances tubes. European Committee for Standardization, junho 2001. EN ISO 10534-2.

[2] Jean-F. Allard and Yvan Champoux. New empirical equations for sound propagation in rigid frame fibrous materials. *Journal of the Acoustical Society of America*, 91(6): 3346–3353, 1992.

[3] L. Cremer. Nachhallzeit und dämpfungsmass bei streifendem einfall. *Akustische Zeitschrift*, 5:57–76, 1940.

[4] A. Cummings. Sound attenuation in ducts lined on two opposite walls with porous material, with some applications to splitters. *Journal of of Sound and Vibration*, 49(1):9–35, 1976.

[5] M.E. Delany and E. N. Bazley. Acoustical properties of fibrous absorvent materials. *Applied Acoustics*, 3:105–116, 1970.

[6] W. Frommhold and F. P. Mechel. Simplified methods to calculate the attenuation of silencers. *Journal of Sound and Vibration*, 141 (1):103–125, 1990.

[7] U. Ingard. On the theory and design of acoustic resonators. *Journal of the Acoustical Society of America*, 25(6):1037–1061, 1953.

[8] U. J. Kurze and I. L. Vér. Sound attenuation in ducts lined with non-isotropic material. *Journal of of Sound and Vibration*, 24(2): 177–187, 1972.

[9] P. M. Morse. The transmission of sound inside pipes. *Journal of the Acoustical Society of America*, 11:205–210, 1940.

[10] D. H. Tack and R. F. Lambert. Influence of shear flow on sound attenuation in a lined duct. *Journal of the Acoustical Society of America*, 38(4):655–666, 1965.